Int. J. Heat Mass Transfer. Vol. 23, pp. 493–504.
Pergamon Press Ltd. 1980. Printed in Great Britain.

GENERAL FEATURES OF CHF OF FORCED CONVECTION BOILING IN UNIFORMLY HEATED VERTICAL TUBES WITH ZERO INLET SUBCOOLING

Y. KATTO
Department of Mechanical Engineering, University of Tokyo,
Hongo, Bunkyo-ku, Tokyo, Japan

(*Received* 15 *June* 1979)

Abstract – In this paper, a graphical method is evolved to give a generalized bird's-eye view of the existing data for critical heat flux (CHF) in vertical tubes with zero inlet subcooling. For this purpose 946 data points obtained from 47 sources are used, including 14 different fluids (water, ammonia, benzene, ethanol, freons, helium I, parahydrogen, monoisopropylbiphenyl, nitrogen, and potassium), tube length from 0.0109 to 8.82 m, tube diameter from 0.00109 to 0.0381 m, and density ratio of vapor/liquid from 0.000270 to 0.413. As a result, a regular nature is elucidated for the CHF under study.

NOMENCLATURE

C, constant, equation (5);
d, I.D. of heated tube [m];
G, mass velocity [$\mathrm{kgm^{-2}\,s^{-1}}$];
H_{fg}, latent heat of evaporation [$\mathrm{Jkg^{-1}}$];
ΔH_i, enthalpy of inlet subcooling [$\mathrm{Jkg^{-1}}$];
K, parameter for the effect of inlet subcooling, equation (1);
l, length of heated tube [m];
q_c, critical heat flux [$\mathrm{Wm^{-2}}$];
q_{co}, q_c for $\Delta H_i = 0$ [$\mathrm{Wm^{-2}}$];
ΔT_i, inlet subcooling temperature [K].

Greek symbols
ρ_l, density of liquid [$\mathrm{kgm^{-3}}$];
ρ_v, density of vapor [$\mathrm{kgm^{-3}}$];
σ, surface tension [$\mathrm{Nm^{-1}}$];
χ, quality (χ_{ex}; exit quality corresponding to critical condition; χ_{in}: inlet quality).

1. INTRODUCTION

RECENTLY, Shah [1] and the present author [2–4] attempted developing generalized correlations of experimental data for critical heat flux (CHF) in uniformly heated vertical tubes. However, a bird's-eye view of CHF data cannot be obtained from these studies, because Shah's graphical correlation was made taking quite different forms for two regions of $Y \lesseqgtr 10^5$ where Y is a dimensionless parameter proportioned to $G^{1.8}$, while the author gave the analysis of CHF data separately for four characteristic regimes called L-, H-, N-, and HP-regime*. This is certainly inconvenient for observing the general features of CHF. In the present paper, therefore, a generalized graphical representation of the existing data is evolved on the basis of the author's correlation principle at a little sacrifice of accuracy.

For the author's correlation [2–4], critical heat flux q_c in case of inlet subcooling enthalpy ΔH_i is written as

$$q_c = q_{co}(1 + K\,\Delta H_i/H_{fg}) \tag{1}$$

and q_{co} on the RHS of equation (1) is correlated in the following form:

$$\frac{q_{co}}{GH_{fg}} = f\left(\frac{\rho_v}{\rho_l}, \frac{\sigma\rho_l}{G^2 l}, \frac{1}{d}\right). \tag{2}$$

Then, according to the preceding study [4], a dimensionless parameter K in equation (1) can be evaluated theoretically in many cases only if the function $f(\ )$ on the RHS of equation (2) is known. Therefore, the correlation of q_{co} alone will be dealt with in this paper.

2. COLLECTION OF q_{co} DATA

2.1. *Method of obtaining* q_{co} *data*

Utilizing actual experimental data from a number of sources [5–52], as listed in Table 1, q_{co} data for pulsation-free upflows are obtained, mostly by the following normal methods (i) and (ii), and partly by some exceptional methods (iii)–(v) to extend the range of experimental conditions.

(i) As for the data providing the variation of q_c with ΔH_i for fixed G, if there are enough data points ($q_c - \Delta H_i$), q_{co} can be obtained by the method of extrapolation (or interpolation, occasionally) as $\Delta H_i \to 0$. The same principle also applies when ΔT_i or χ_{in} is used instead of ΔH_i. In the special case of experiment made with ΔH_i which is zero substantially, q_{co} can be obtained immediately from the data.

(ii) As for the data providing the variation of q_c with χ_{ex} for fixed G, the relation of q_c vs ΔH_i can be derived through the well-known heat balance equation for uniformly heated tubes:

* In a rough sense, it seems that Shah's region of $Y < 10^5$ corresponds to Katto's L-regime while $Y > 10^5$ to other three regimes.

Table 1. Summary of the collected data of q_{co}

Source	Fluid	l (cm)	d (cm)	l/d	$(\rho_v/\rho_l) \times 10^2$	$\sigma\rho_l/G^2l$	No. of Data
Lowdermilk *et al.* [5]	Water	12.9–48.6	0.129–0.243	100–200	0.0623	3.42×10^{-5}–6.82×10^{-4}	7
Aladyev *et al.* [6]	Water	16.0	0.800	20	7.82	3.19×10^{-4}	1
Lee-Obertelli [7]	Water	43.2–366	1.08	40–338	4.81	7.79×10^{-7}–6.60×10^{-6}	5
Matzner [8]	Water	198	0.558–3.75	52–359	4.81	1.45×10^{-6}–1.89×10^{-6}	7
Weatherhead [9]	Water	45.7	0.772	59	13.5	1.26×10^{-6} 1.01×10^{-5}	3
Barnett [10]	Water	178	1.27–3.81	47–140	4.81	3.01×10^{-6}	2
Bergles [11]	Water	1.19–11.4	0.118–0.458	5.0–25	1.24	1.36×10^{-5}–5.22×10^{-4}	12
Thompson–Macbeth [12]	Water	15.2–365	0.304–3.74	26–358	0.0623–13.5	2.14×10^{-7}–9.30×10^{-1}	81
Thompson–Macbeth [13]	Water	8.51–312	0.170–1.00	50–792	0.0623–13.5	7.11×10^{-6}–1.00×10^{0}	139
Matzner *et al.* [14]	Water	244–488	1.02	240–480	4.84	2.90×10^{-8}–2.43×10^{-6}	15
Hewitt *et al.* [15]	Water	121	0.929	131	0.0736–0.122	4.72×10^{-4}–3.16×10^{-3}	3
Lee [16]	Water	63.5–152	1.40–2.82	42–108	6.51–11.2	4.58×10^{-7}–4.67×10^{-5}	38
Bennett *et al.* [17]	Water	144	1.25	290	4.81	4.74×10^{-7}–1.89×10^{-6}	2
Bennett *et al.* [18]	Water	342–416	1.26	271–330	4.81	1.16×10^{-7}–2.38×10^{-5}	36
Barbarin *et al.* [19]	Water	96.0–180	1.20	80–150	0.173	1.33×10^{-4}–1.99×10^{-2}	26
Hewitt [20]	Water	580	0.617	940	4.81	1.33×10^{-7}–2.98×10^{-7}	2
Sterman–Nekrasov [21]	Water	37.0–50.0	0.800	46–62	1.78	1.40×10^{-5}–6.73×10^{-5}	4
Ornatskii *et al.* [22]	Water	8.70–44.0	0.290–0.800	30–150	1.79–7.82	7.80×10^{-4}–1.66×10^{-3}	8
Midler–Shitsman [23]	Water	321	1.00	321	8.05	7.96×10^{-6}	1
Roko *et al.* [24]	Water	360	1.25	288	2.53	5.12×10^{-5}	1
Doroshchuk *et al.* [25, 26]	Water	150	0.800	188	3.19–27.1	1.50×10^{-7}–1.14×10^{-5}	27
Peskov *et al.* [27]	Water	165	0.800	206	36.1	2.73×10^{-8}	1
Becker *et al.* [28]	Water	200–500	1.00	200–500	14.0–34.7	2.78×10^{-9}–6.47×10^{-7}	83
Chojnowski–Wilson [29]	Water	762	3.20	238	24.3	8.43×10^{-8}–3.90×10^{-7}	4
Watson *et al.* [30]	Water	549	3.78	145	27.1	4.68×10^{-8}–1.17×10^{-6}	6

Table 1. – *continued*

Source	Fluid	l (cm)	d (cm)	l/d	$(\rho_v/\rho_l) \times 10^2$	$\sigma\rho_l/G^2l$	No. of Data
Noel [31]	Ammonia*	8.00	0.589	14	5.26	8.20×10^{-7}–3.13×10^{-6}	2
Sterman *et al.* [32]	Benzene	10.0	1.00	10	0.675	1.55×10^{-6}–1.40×10^{-5}	3
Pokhalov *et al.* [33]	Benzene	8.00	0.500	16	0.978–14.3	1.08×10^{-7}–2.65×10^{-5}	10
Tolubinskiy–Matorin [34]	Benzene	6.00	0.400	15	2.37	1.10×10^{-5}	1
Tolubinskiy–Matorin [34]	Ethanol	6.00	0.400	15	1.49	1.17×10^{-5}	1
Giarratano *et al.* [35]	He†	1.09–7.64	0.213	5.1–36	15.1–21.1	2.72×10^{-7}–1.10×10^{-5}	9
Keilin *et al.* [36]	He†	10.0	0.200	50	17.0	6.04×10^{-5}	1
Ogata-Sato [37]	He†	2.80–5.60	0.109	26–51	15.1–41.3	2.90×10^{-6}–5.00×10^{-5}	10
Lewis *et al.* [38]	H_2‡	28.0–40.6	1.40	20–29	6.34–7.10	3.72×10^{-4}–7.74×10^{-3}	21
Sterman *et al.* [32]	MIPD§	10.0	1.00	10	1.03	1.23×10^{-6}–1.10×10^{-5}	3
Lewis *et al.* [38]	N_2	40.6	1.40	29	1.78–1.97	2.16×10^{-3}–2.61×10^{-2}	11
Papell [39]	N_2	30.5	1.28	24	3.00–6.52	1.39×10^{-6}–1.93×10^{-6}	3
Stevens *et al.* [40]	R-12	24.1–357	0.525–1.61	28–337	4.82	2.37×10^{-7}–3.80×10^{-4}	102
Stevens *et al.* [41]	R-12	32.4–259	0.965	33–268	4.82	9.52×10^{-7}–6.10×10^{-5}	11
Barnett-Wood [42]	R-12	43.9–241	0.770–0.965	57–313	2.41–4.81	7.91×10^{-7}–1.00×10^{-4}	31
Groeneveld [43]	R-12	138	0.780	177	4.98	8.47×10^{-8}–3.14×10^{-6}	6
Cumo *et al.* [44]	R-12	200	0.780	256	4.97–9.88	1.96×10^{-6}–1.97×10^{-4}	17
Barnett–Wood [42]	R-21	52.8–331	0.671–1.61	76–318	2.40–4.85	6.17×10^{-7}–9.37×10^{-5}	100
Staub [45]	R-22	152	1.02	150	2.10–4.82	1.99×10^{-6}–3.71×10^{-5}	32
Coffield *et al.* [46]	R-113	76.2	1.02	75	4.89–13.9	1.15×10^{-7}–1.84×10^{-6}	4
Ueda *et al.* [47, 48]	R-113	254–882	1.00	254–882	1.47	2.20×10^{-6}–6.17×10^{-5}	9
Dix [49]	R-114	91.4–150	0.998–1.41	65–150	4.85–8.46	1.62×10^{-6}–3.97×10^{-5}	19
Hoffman–Krakoviak [50]	K	37.1–183	0.825–2.21	45–83	0.0820	2.67×10^{-3}–5.11×10^{-3}	6
Bond–Converse [51]	K	87.1–612	1.07–1.94	45–569	0.526–0.953	4.42×10^{-5}–2.89×10^{-3}	16
Akad'yev *et al.* [52]	K	12.0–40.0	0.400–0.600	30–100	0.0270–0.336	1.88×10^{-3}–2.87×10^{-2}	4
							Total 946

* Anhydrous ammonia.
† Helium I.
‡ Para-hydrogen.
§ Monoisopropylbiphenyl.

$$\frac{4q_c}{GH_{fg}}\frac{l}{d}-\frac{\Delta H_i}{H_{fg}}=\chi_{ex}. \tag{3}$$

Therefore, the method (i) is applicable. In this case, however, there are occasionally papers giving q_c only for high degree mixed-inlet-condition ($\Delta H_i < 0$), and the presumption of q_{co} as $\Delta H_i \to 0$ from such data is avoided because of the ambiguity of the flow pattern given at the tube inlet.

(iii) References [18, 24, 35] give the data of sharp wall-temperature rise position for subcooled or saturated inlet condition ($\Delta H_i \geqq 0$). In this case, if the axial length between the above-mentioned temperature rise position and the computed position of $\chi = 0$ is taken as l, the experimental CHF is regarded as q_{co}.

(iv) References [47, 48, 51] give the data of sharp wall-temperature rise position for mixed inlet condition ($\Delta H_i < 0$). In this case, the l determined by means of the method (iii) becomes an imaginary length, but the preceding study [4] has shown that the above-mentionled l can be used to correlate data without serious error so far as L-regime (see Section 3.2) is concerned.

(v) References [13, 45] give the data for independent sets of G, ΔH_i and q_c. Therefore, q_{co} is estimated through equation (1) with semi-theoretical value of K derived in the preceding study [4]. In this case, if the value of $K\Delta H_i/H_{fg}$ is small compared with unity, serious error does not arise for the estimation of q_{co}. To supplement the data in L-regime [13] is used while [45] provides the data of R-22 in H-regime.

2.2. *Note on the data*

The data of [7–10] are those referred to by Collier in his book [59] while the data of [11] are those referred to by Rohsenow in *Handbook of Heat Transfer* [60]. As for [15], the data of thick-walled tube in Fig. 2.9 are used. For [21] the data for $l = 1.57$ m are discarded due to considerable scatter of data, and for [25, 26] actual experimental data shown in graphs are utilized, discarding recommended CHF values which assume non-influence of l and of inlet parameters for $l/d > 20$ (N.B. 493 data points from the latter were used in the correlation of Shah [1]). As for [27], only one data at $p = 200$ atm is utilized due to the scarcity of data for fixed G. In [35], the data in case of $\Delta H_i = 0$ alone are used for simplicity. Miscopies found in tabulation of [45] and [49] have been corrected (cf. [2] and [3]).

As was mentioned in [2, 3] as VL-regime, it seems likely that if l/d is small and if the inlet velocity is very low, ordinary pool boiling is apt to prevail. From this point of view, the data of [33] in the range of $\sigma\rho_l/G^2 l > 3 \times 10^{-5}$ (cf. Fig. 10 of [3]) and a part of H_2 data of [38] (cf. Fig. 9 of [2]) have been discarded. For the same reason, among the data of [39], upflow data at the highest velocity (3.5 m/s) alone are adopted for information. The data of Cheng and Ng [53] are not considered, because they are clearly in the regime suffering the effect of pool boiling.

Finally, the data of Borishansky *et al.* [54], Doroshchuk and Lantsman [55], and Smolin [56] cannot be utilized due to the lack of information of l. Eliminations of data other than those mentioned in this Section have not been made in the present study except those cases with clear reasons such as unstable flow, anomalous condition, etc.

3. GRAPHIC REPRESENTATION OF q_{co} DATA

3.1. *Representation of q_{co} data*

The experimental data of q_{co} collected in Section 2 are listed in Table 1 along with the kind of fluid, the range of experimental conditions, and the number of collected data, where physical properties for monoisopropylbiphenyl alone are those estimated by the method of [57, 58]. Then, assuming the possibility of correlating the data in the form of equation (2), 13 graphs are prepared for distinct values of l/d as shown in Fig. 1, and the data of q_{co}/GH_{fg} are plotted against $\sigma\rho_l/G^2 l$ (the division of data by l/d to each graph and the treatment of ρ_v/ρ_l effect will be explained in Section 3.3). Data symbols shown in Table 2 are used in Fig. 1 to discriminate the kind of fluid. When many data gather together to the same place, plotting a part of data is eliminated to avoid the confusion.

3.2. *Representation of the author's correlation equations*

Based on the results of the preceding study [2, 3], the characteristic regimes L, H, N, and HP, the correlation curves (a) to (e), and the boundary (f) between H- and N-regime are shown in Fig. 1 applying the following equations:

Table 2. Symbols used to specify the fluids in Fig. 1

Ref. no.	Fluid	Symbol	Ref. no.	Fluid	Symbol
5–24	Water	○	32	MIPB	⊟
25, 26	Water	◐	38, 39	N_2	■
27	Water	◪	40–44	R-12	△
28–30	Water	●	42	R-21	▽
31	Ammonia	⊖	45	R-22	□
32–34	Benzene	⊖	46–48	R-113	▲
34	Ethanol	⊖	49	R-114	▽
35–37	He	+	50–52	K	×
38	H_2	●			

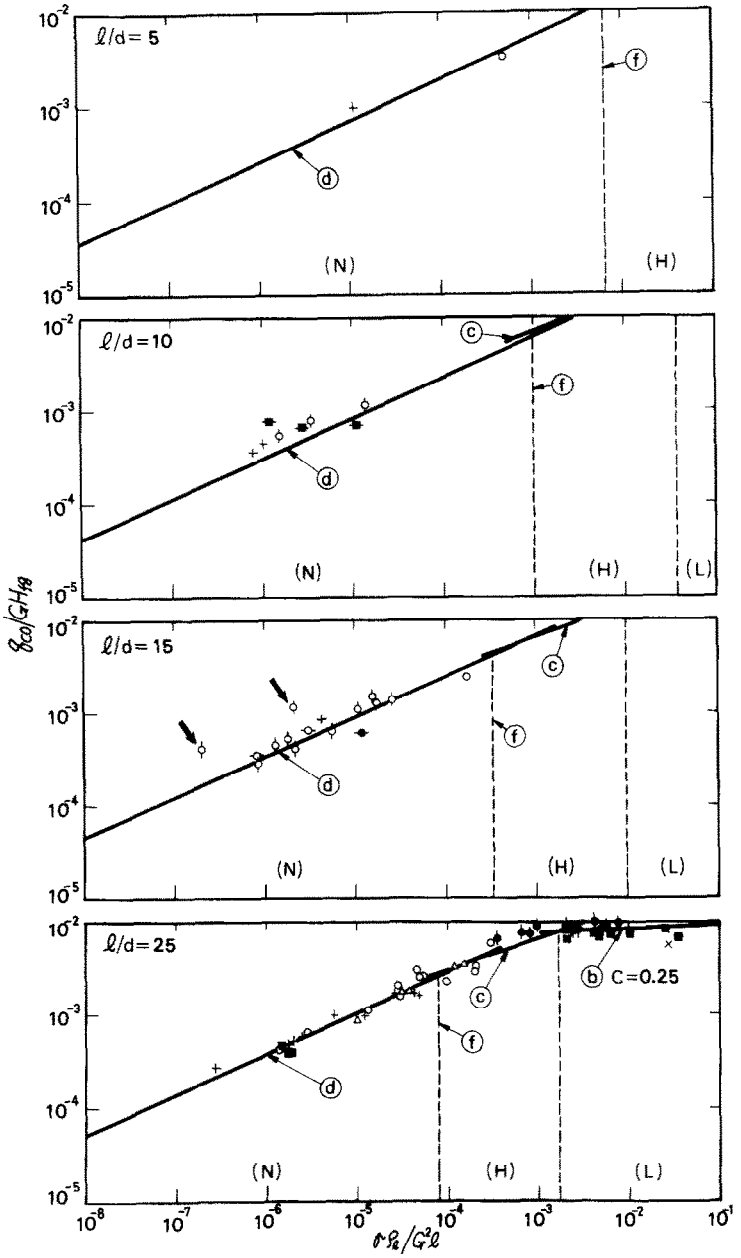

FIG. 1. Generalized graphic representation of q_{co} data. (L): L-regime, (H): H-regime, (N): N-regime, (HP): HP-regime, a: equation (4), b: equation (5), c: equation (6) with $\rho_v/\rho_l = 0.048$, d: equation (7) with $\rho_v/\rho_l = 0.048$, e: equation (8), f: equation (9).

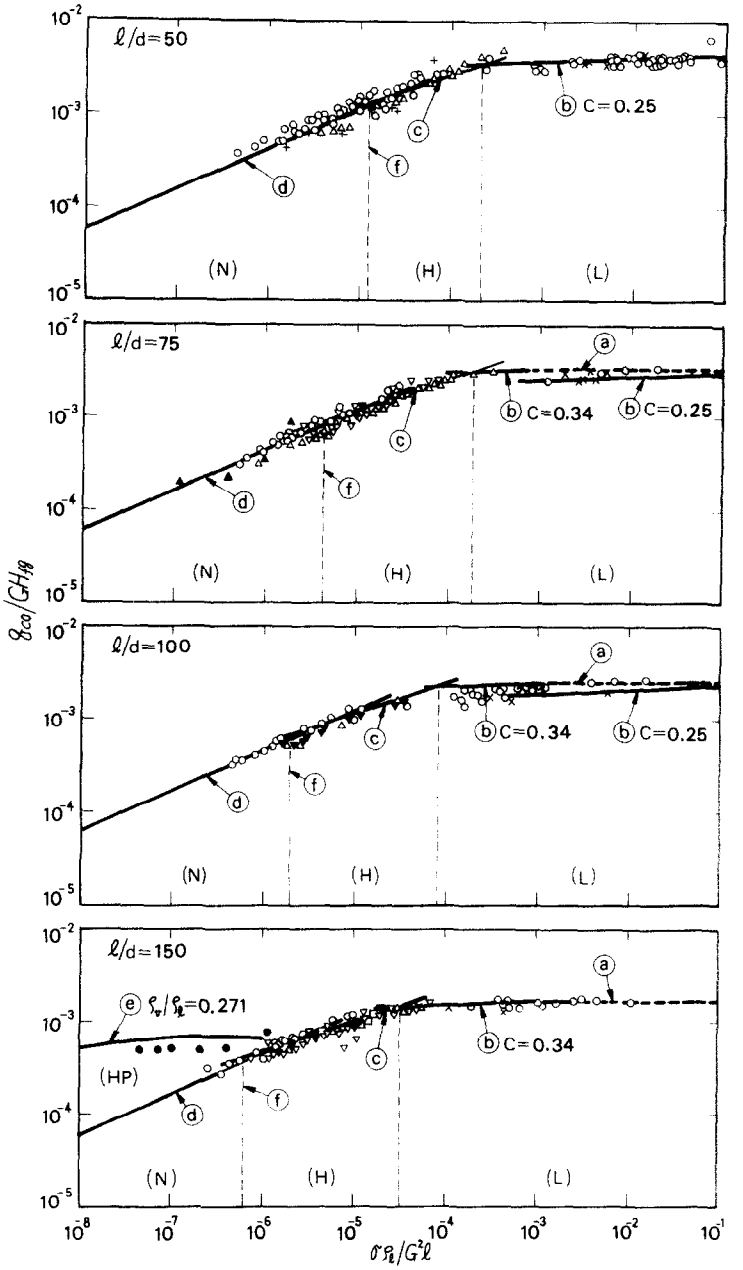

FIG. 1.—continued.

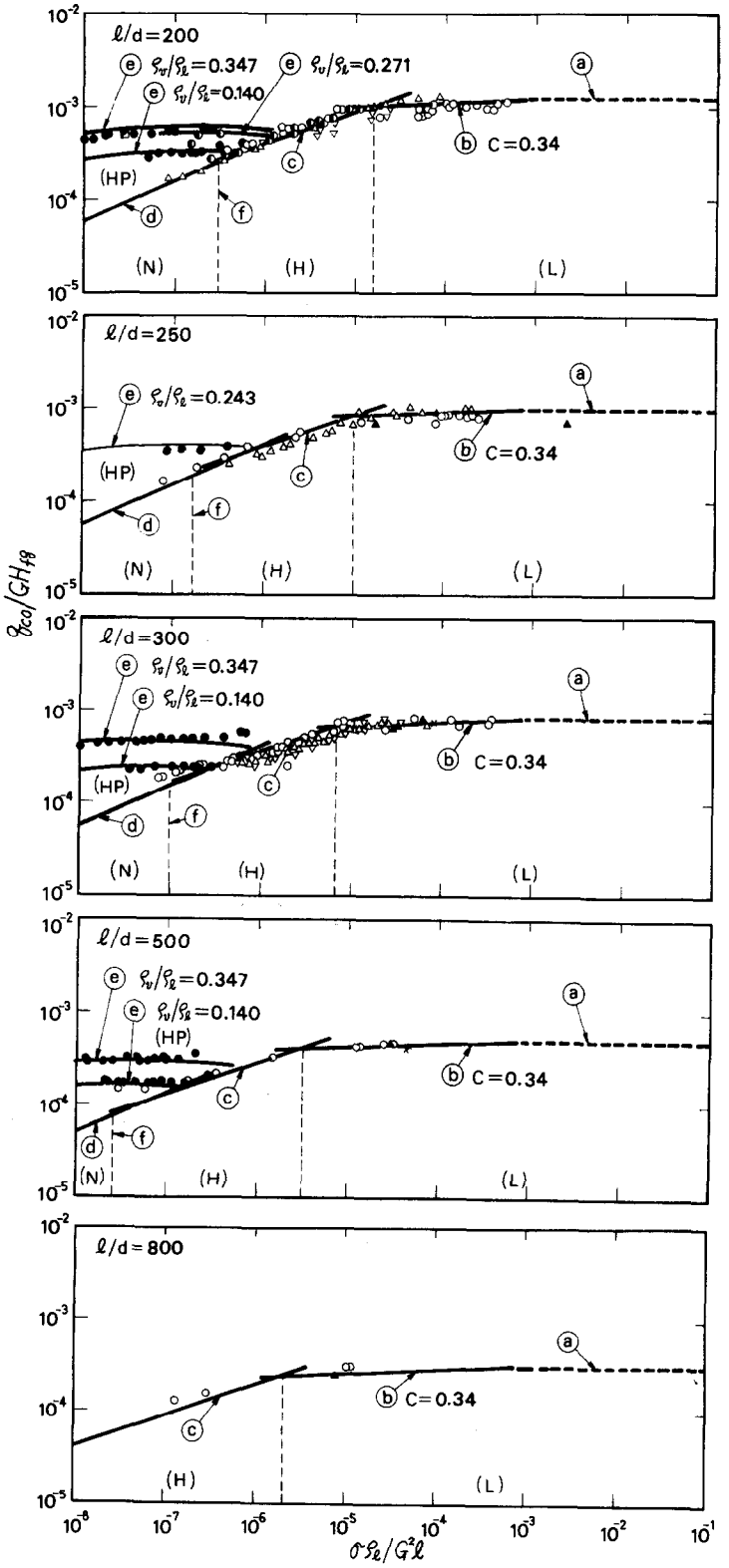

FIG. 1.—continued.

Table 3. Experimental range of l/d and ρ_v/ρ_l in each regime for the data of Fig. 1, excluding the data of Table 4

Nominal $\frac{l}{d}$	HP-regime $\frac{l}{d}$	HP-regime $\frac{\rho_v}{\rho_l} \times 10^2$	H and N-regime $\frac{l}{d}$	H and N-regime $\frac{\rho_v}{\rho_l} \times 10^2$	L-regime $\frac{l}{d}$	L-regime $\frac{\rho_v}{\rho_l} \times 10^2$	Ref. no. *
10	—	—	10.0	1.03	—	—	32
15	—	—	13.6–16.0	0.979–6.42	—	—	31, 33, 34
25	—	—	20.0–33.4	1.79–7.82	20.0–30.0	0.105–7.10	6, 12, 22, 38, 39, 40, 41, 52
50	—	—	39.2–59.2	1.79–13.5	40.2–60.1	0.0623–13.5	7, 8, 9, 10, 12, 13, 16, 21, 22, 35, 40, 42, 50, 51, 52
75	—	—	67.0–83.5	2.41–11.2	62.5–83.0	0.0820–4.82	7, 8, 12, 16, 19, 21, 40, 41, 42, 46, 49, 50, 52
100	—	—	90.2–112	1.79–11.2	86.8–105	0.0270–2.07	5, 12, 13, 16, 19, 22, 40, 42, 49, 51, 52
150	145	27.1	123–161	1.79–9.28	123–159	0.0736–4.85	7, 8, 10, 12, 13, 15, 19, 22, 30, 40, 41, 42, 45, 49, 51
200	188–206	14.0–36.1	175–214	2.41–13.1	178–224	0.0623–4.82	5, 8, 12, 13, 25, 25, 26, 26, 27, 28, 40, 42, 43, 51
250	238	24.3	229–268	4.84–9.88	249–268	0.404–9.81	12, 13, 14, 29, 29, 41, 44, 47, 48
300	300	14.0–34.7	271–360	2.40–8.05	286–337	0.293–4.86	7, 8, 12, 13, 14, 17, 18, 23, 24, 28, 40, 42, 47, 48, 51
500	500	14.0–34.7	480	4.84	528–569	0.614–2.28	13, 14, 28, 47, 48, 51
800	—	—	940	4.81	792–882	1.47–2.21	13, 20, 47, 48

* Italic numbers indicate the references which give HP-regime data.

L-regime,

$$\text{(a)}: \quad \frac{q_{co}}{GH_{fg}} = 0.25\frac{1}{l/d}, \quad \text{or} \quad \chi_{ex} = 1 \tag{4}$$

$$\text{(b)}: \quad \frac{q_{co}}{GH_{fg}} = C\left(\frac{\sigma\rho_l}{G^2 l}\right)^{0.043}\frac{1}{l/d} \tag{5}$$

where

$$C = 0.25 \quad \text{or} \quad 0.34.$$

H- and N-regime,

$$\text{(c)}: \quad \frac{q_{co}}{GH_{fg}} = 0.10\left(\frac{\rho_v}{\rho_l}\right)^{0.133}\left(\frac{\sigma\rho_l}{G^2 l}\right)^{1/3} \times \frac{1}{1 + 0.0031\, l/d} \tag{6}$$

where

$$\rho_v/\rho_l = 0.048 \text{ for (c).}$$

$$\text{(d)}: \quad \frac{q_{co}}{GH_{fg}} = 0.098\left(\frac{\rho_v}{\rho_l}\right)^{0.133}\left(\frac{\sigma\rho_l}{G^2 l}\right)^{0.433} \times \frac{(l/d)^{0.27}}{1 + 0.0031\, l/d} \tag{7}$$

where

$$\rho_v/\rho_l = 0.048 \text{ for (d).}$$

HP-regime,

$$\text{(e)}: \quad \frac{q_{co}}{GH_{fg}} = 8.20\left(\frac{\rho_v}{\rho_l}\right)^{0.65}\left(\frac{\sigma\rho_l}{G^2 l}\right)^{0.453} \times \frac{1}{1 + 107\left(\frac{\sigma\rho_l}{G^2 l}\right)^{0.54}\frac{l}{d}}. \tag{8}$$

Boundary between H- and N-regime,

$$\text{(f)}: \quad \frac{\sigma\rho_l}{G^2 l} = \left(\frac{0.77}{l/d}\right)^{2.70} \tag{9}$$

In Fig. 1, the lines (a) and (b) for L-regime are given independently of ρ_v/ρ_l [see equations (4) and (5)]. The intersecting point between (a) and (b) appears at

$$\sigma\rho_l/G^2 l = 7.84 \times 10^{-4} \tag{10}$$

which is determined by eliminating q_{co} from equations (4) and (5) with $C = 0.34$ for $l/d = 75$–800 as seen in Fig. 1. Next, the lines (c) and (d) for H- and N-regime in Fig. 1 show the prediction of equations (6) and (7) in case of $\rho_v/\rho_l = 0.048$ corresponding to saturated steam and water at 68.5 bars for example. It should be noted that l/d does not exert its influence on the lines (c) and (d) so much as on the lines (a) and (b) [cf. equations (4)–(7)]. Finally, the curves (e) for HP-regime of Fig. 1 show the prediction of equation (8) for $\rho_v/\rho_l = 0.140$, 0.234, 0.271, and 0.347.

3.3. *Effects of* ρ_v/ρ_l

The data points plotted in Fig. 1 can be classified according to the regimes of L, H + N, and HP determined in Fig. 1, yielding the result of Table 3 with the range of l/d and ρ_v/ρ_l covered in each data set, on the condition that a small number of data in the regime of H + N with comparative high or low values of ρ_v/ρ_l are omitted from Table 3 to be shown in Table 4.

Now, as for L-regime data in Table 3, it is noted that the value of ρ_v/ρ_l shows a variation as much as 500 times ($= 13.5 \div 0.0270$). However, the data points of CHF plotted in L-regime in Fig. 1 show no mutual discrepancies owing to the difference of ρ_v/ρ_l, and this independence of ρ_v/ρ_l agrees with the character of equations (4) and (5).

Table 4. Data with comparatively high or low values of ρ_v/ρ_l in H and N-regime

Nominal $\frac{l}{d}$	H and N-regime $\frac{l}{d}$	$\frac{\rho_v}{\rho_l} \times 10^2$	No. of data	Ref. no.
5	5.0	0.124	2	[11]
	5.14	15.1	1	[35]
10	7.86–10.9	21.1	2	[35]
	10.0	0.675	3	[32]
15	15.0	0.124	1	[11]
	12.5	0.151	1	[35]
25	25.0	0.124	9	[11]
	21.8–31.2	15.1–21.1	4	[35]
	25.7	15.1–41.3	5	[37]
50	35.9	15.1	1	[35]
	50.0	17.0	1	[36]
	51.4	15.1–41.3	5	[37]
200	188	15.4–20.1	7	[25, 26]
			Total 42	

Next, H- and N-regime data in Table 3 change the value of ρ_v/ρ_l in some degree above and below the value of 0.048 (cf. Section 3.2). However, the data points of CHF plotted in H- and N-regime in Fig. 1 appear along by the lines (c) and (d), supporting equations (6) and (7) on the point that the effect of ρ_v/ρ_l on CHF is only in the degree of $(\rho_v/\rho_l)^{0.133}$. It should be noted here that correction of experimental value of q_{co} by $(\rho_v/\rho_l)^{0.133}$ in plotting the data in Fig. 1 has not been done, mainly because of avoiding artificial modification of data as far as possible, and partly because of the difficulty of dealing with the data near the boundary between L- and H-regime with different character as to the effect of ρ_v/ρ_l. However, the correction of multiplying $[0.048/(\rho_v/\rho_l)]^{0.133}$ to q_{co}/GH_{fg} has been made for the small number of data of Table 4, because the difference of ρ_v/ρ_l from 0.048 is comparatively large and the data are sufficiently apart from L-regime.

Finally, HP-regime data in Table 3 are subject to a strong influence of ρ_v/ρ_l as is noticed in Fig. 1, so that the curve (e) representing the prediction of equation (7) is drawn in Fig. 1 for every experimental value of ρ_v/ρ_l on the condition that $\rho_v/\rho_l = 0.361$, which corresponds to only one data of water [27], is omitted for avoiding the confusion of representation.

4. DISCUSSION OF THE RESULT OF FIG. 1

(I) It is of interest to know that a large number of q_{co} data obtained from various independent sources [5–52] indicates such a regular nature as shown in Fig. 1 for a wide range of l/d, suggesting the importance of the dimensionless group $\sigma\rho_l/G^2l$ for this phenomenon, (N.B. the comparative deviation of two benzene data for $l/d = 15$, indicated by thick arrows in Fig. 1, is unaccountable as was mentioned in the preceding study [3]). In connection with this point, it may be of use to add that this type of dimensionless group, which is composed with the length of heated surface measured in the direction of forced convection, can play an important role for correlating CHF in forced flow of a jet over a heated surface [61–64].

(II) It may be said from the result of Fig. 1 that the author's correlation equations (4)–(8) express the general trend of experimental data on the whole.

(III) In the author's preceding study [3], the constant C in equation (5) was tentatively determined as $C = 0.25$ for $5 \times 10^{-4} < \sigma\rho_l/G^2l$ and $C = 0.34$ for $\sigma\rho_l/G^2l < 5 \times 10^{-4}$, and this character is fairly observed in Fig. 1, too. However, a detailed observation of Fig. 1 reveals a better formulation that $C = 0.25$, for $l/d < 50$, $C = 0.34$ for $l/d > 150$, and a transition between $C = 0.25$ and $C = 0.34$ takes place in the range of $l/d \simeq 75$–100.

(IV) Correlation equation (8) for q_{co} in HP-regime agrees with experimental data fairly well as shown in Fig. 13 of [2]. However, there is still an anxious matter found in [4] that the parameter K_{HP} for the effect of inlet subcooling on CHF in HP-regime derived theoretically from equation (8) is slightly higher than the experimental data of K_{HP}. Therefore, it is naturally impossible to derive the ultimate criterion for the onset of HP-regime from the result of Fig. 1 based on equation (8). However, it may not be useless for the present to give the following tentative criterion. If it is assumed that the curve (e) of HP-regime in Fig. 1 can appear only originating itself on the line (c) of H-regime*, the lowest value of ρ_v/ρ_l for permitting the onset of HP-regime occurs when the intersecting point between (e) and (c) [determined by eliminating q_{co}/GH_{fg} from equations (6) and (8)] agrees with the intersecting point between (c) and (d) [determined by eliminating q_{co}/GH_{fg} from equations (6) and (7)] to give

$$\frac{\rho_v}{\rho_l} = \left[\frac{116(l/d)^{-0.134} + 0.976(l/d)^{0.324}}{0.254(l/d) + 82}\right]^{1.93}, \qquad (11)$$

and Table 5 shows the computed result of equation (11).

Then, the circumstances for the appearance of HP-regime in Fig. 1 are explained as follows. First, CHF in HP-regime is not observed for $l/d = 25$ and 50 in Fig. 1 in spite of the experimental value of ρ_v/ρ_l as much as 0.413 (see Table 4), but it is natural because the lowest values of ρ_v/ρ_l given in Table 5 for $l/d = 25$ and 50 are much larger than 0.413. On the other hand, HP-regime is observed for $l/d = 150$–500 in Fig. 1, and it is also natural because the values of ρ_v/ρ_l listed in the column of HP-regime in Table 3 are on the whole larger than the respective lowest values of ρ_v/ρ_l in Table 5, though some minor discrepancies are observed.

* Notice that the H–HP boundary defined by equation (19) of the preceding study [2] is kept unchanged.

Table 5. Lowest limit of ρ_v/ρ_l for the appearance of CHF in HP-regime

l/d	5	10	15	25	50	75	100	150	200	250	300	500	800
$\rho_v/\rho_l \times 10^2$	129*	106*	93.8	78.8	59.0	47.8	40.0	29.8	23.2	18.7	15.4	8.31	4.27

* Values of $\rho_v/\rho_l > 1.0$ mean nonexistence of HP-regime.

(V) It is noticed in Fig. 1 that experimental data of freons have a trend to be slightly lower than those of water in H- and N-regime for $l/d \geqq 50$. This trend coincides with the indication given in the preceding paper [3] (see the discussion of mass flux scaling factor). It is also noticed in Fig. 1 that experimental data in H-regime for $l/d \geqq 250$ seem to have slower gradient than the line (c). In addition, it should be mentioned that the data of potassium exist in L-regime alone, while the data for HP-regime are only of water.

5. CONCLUDING REMARKS

Dealing with CHF of forced convection boiling in uniformly heated tubes with zero inlet subcooling, a generalized graphical representation of 946 data points listed in Table 1 has been made giving the result of Fig. 1, and thereby the following quantitative informations are obtained: (a) the behavior of constant C in equation (5) as described in Section 4(III), and (b) the lowest value of ρ_v/ρ_l for the onset of HP-regime as given by equation (11).

Acknowledgements – I would like to pay my respects to all the authors reporting the experimental data used in this paper, and the financial support given by the Ministry of Education, Science and Culture to this study under Grant in Aid of Special Project Research No. 411002 (1979) is gratefully acknowledged.

REFERENCES

1. M. M. Shah, A generalized graphical method for predicting CHF in uniformly heated vertical tubes, *Int. J. Heat Mass Transfer* **22,** 557–568 (1979).
2. Y. Katto, A generalized correlation of critical heat flux for the forced convection boiling in vertical uniformly heated round tubes, *Int. J. Heat Mass Transfer* **21,** 1527–1542 (1978).
3. Y. Katto, A generalized correlation of critical heat flux for the forced convection boiling in vertical uniformly heated round tubes – a supplementary report, *Int. J. Heat Mass Transfer* **22,** 783–794 (1979).
4. Y. Katto, An analysis of the effect of inlet subcooling on critical heat flux of forced convection boiling in vertical uniformly heated tubes, *Int. J. Heat Mass Transfer* **22,** 1567–1575 (1979).
5. W. H. Lowdermilk, C. D. Lanzo and B. L. Siegel, Investigation of boiling burnout and flow stability for water flowing in tubes (Table IV), NACA TN 4382 (1958).
6. I. T. Aladyev, Z. L. Miropolsky, V. E. Doroshchuk and M. A. Styrikovich, Boiling crisis in tubes, in *International Developments in Heat Transfer*, pp. 237–243. ASME, New York (1961).
7. D. H. Lee and J. D. Obertelli, An experimental investigation of forced convection boiling in high pressure water, Part 1, UKAEA, AEEW-R 213 (1963).
8. B. Matzner, Basic experimental studies of boiling fluid flow and heat transfer at elevated pressure, T.I.D.18978 (1963).
9. R. J. Weatherhead, Nucleate boiling characteristics and the critical heat flux occurrence in sub-cooled axial-flow water systems, A.N.L.6675 (1963).
10. P. G. Barnett, The relevance of burnout in uniformly heated round tubes to burnout in non-uniformly heated reactor channels, UKAEA, AEEW-R 362 (1964).
11. A. E. Bergles, Forced convection surface boiling heat transfer and burnout in tubes of small diameter, Doctoral dissertation, MIT (1962).
12. B. Thompson and R. V. Macbeth, Boiling water heat transfer burnout in uniformly heated round tubes: a compilation of world data with accurate correlations (Tables 1–10), UKAEA, AEEW-R 356 (1964).
13. B. Thompson and R. V. Macbeth, Boiling water heat transfer burnout in uniformly heated round tubes: a compilation of world data with accurate correlations (Table 15 mainly, and Tables 1, 2, 4, 5, 6, 10), UKAEA, AEEW-R 356 (1964).
14. B. Matzner, J. E. Casterline, E. O. Moeck and G. A. Wikhammer, Critical heat flux in long tubes at 1000 psi with and without swirl promoters, ASME Paper No. 65-WA/HT-30 (1965).
15. G. F. Hewitt, H. A. Kearsey, P. M. C. Lacey and D. J. Pulling, Burn-out and film flow in the evaporation of water in tubes, *Proc. Instn Mech. Engrs* **180** (3C), 206–215 (1965–66).
16. D. H. Lee, An experimental investigation of forced convection burnout in high pressure water (Part IV, Large diameter tubes at about 1600 psi), UKAEA, AEEW-R 479 (1966).
17. A. W. Bennett, G. F. Hewitt, H. A. Kearsey, R. K. F. Keeys and D. J. Pulling, Studies of burnout in boiling heat transfer, *Trans. Instn. Chem. Engrs* **45,** T319–T333 (1967).
18. A. W. Bennett, G. F. Hewitt, H. A. Kearsey and R. K. F. Keeys, Heat transfer to steam-water mixtures flowing in uniformly heated tubes in which the critical heat flux has been exceeded, UKAEA, AERE-R 5373 (1967).
19. V. P. Babarin, R. I. Sevast'yanov and I. T. Alad'yev, A special hydrodynamic effect on the boiling crisis in tubes, *Heat Transfer—Soviet Res.* **1**(4), 34–41 (1969).
20. G. F. Hewitt, Experimental studies on the mechanism of burnout in heat transfer to steam-water mixtures, in *Heat Transfer 1970*, Vol. VI, B.6.6. Elsevier, Amsterdam (1970).
21. L. S. Sterman and A. V. Nekrasov, Studies of burnout heat fluxes with water boiling in tubes, in *Heat Transfer 1970*, Vol. VI, B.6.9. Elsevier, Amsterdam (1970).
22. A. P. Ornatskii, L. F. Gluschchenko and E. M. Maevskii, Critical heat flux in steam generating tubes in the region of low subcooling and steam content, *Therm. Engng* **18** (8), 106–109 (1971).
23. L. S. Midler and M. Ye. Shitsman, Effect of sodium chloride addition in boiling crisis in up- or down-flow of water, *Heat Transfer—Soviet Res.* **9**(2), 1–4 (1977).
24. K. Roko, K. Takitani, A. Yoshizaki and M. Shiraha, Dryout characteristics at low mass velocities in a vertical straight tube of a steam generator, in *Heat Transfer 1978*, Vol. 1, pp. 429–434. Hemisphere, Washington (1978).
25. V. E. Doroschuk, L. L. Levitan and F. P. Lantzman, Investigation into burnout in uniformly heated tubes,

ASME Paper No. 75-WA/HT-22 (1975).
26. L. L. Levitan and F. P. Lantzman, Investigating burnout with flow of a steam–water mixture in a round tube, *Therm. Engng* **22**(1), 102–105 (1975).
27. O. L. Peskov, V. I. Subbotin, B. A. Zenkevich and N. D. Sergeyev, The critical heat flux for the flow of steam–water mixtures through pipes, in *Problems of Heat Transfer and Hydraulics of Two-phase Media*, pp. 48–62 (edited by S. S. Kutateladze). Pergamon Press, Oxford (1969).
28. K. M. Becker, D. Djursing, K. Lindberg, O. Eklind and C. Österdahl, Burnout conditions for round tubes at elevated pressures, in *Progress in Heat and Mass Transfer*, Vol. 6, pp. 55–74. Pergamon Press, Oxford (1972).
29. B. Chojnowski and P. W. Wilson, Critical heat flux for large diameter steam generating tubes with circumferentially variable and uniform heating, *Heat Transfer 1974*, Vol. IV, pp. 260–264. Hemisphere, Washington (1974).
30. G. B. Watson and R. A. Lee, Critical heat flux in inclined and vertical smooth and ribbed tubes, *Heat Transfer 1974*, Vol. IV, pp. 275–279. Hemisphere, Washington (1974).
31. M. B. Noel, Experimental investigation of the forced convection and nucleate boiling heat transfer characteristics of liquid ammonia, C.I.T., JPL Tech. Report No. 32–125 (1961).
32. L. Sterman. A. Abramov and G. Checheta, Investigation of boiling crisis at forced motion of high temperature organic heat carriers and mixtures, in *Cocurrent Gas–Liquid Flow*, pp. 455–470. Plenum Press, New York (1969).
33. Yu. Ye. Pokhvalov, I. V. Kronin and S. V. Yermakov, Critical heat fluxes in benzene boiling at saturation temperature, *Heat Transfer—Soviet Res.* **3**(1), 23–29 (1971).
34. V. I. Tolubinskiy and A. S. Matorin, Forced convection boiling heat transfer crisis with binary mixtures, *Heat Transfer—Soviet Res.* **5**(2), 98–101 (1973).
35. P. J. Giarratano, R. C. Hess and M. C. Jones, Forced convection heat transfer to subcritical helium I, *Adv. Cryogen. Engng* **19**, 404–416 (1974).
36. V. E. Keilin, I. A. Kovalev, V. V. Likov and M. M. Pozvonkov, Forced convection heat transfer to liquid helium I in the nucleate boiling region, *Cryogenics* **15**, 141–145 (1975).
37. H. Ogata and S. Sato, Critical heat flux for two-phase flow of helium I, *Cryogenics* **13**, 610–611 (1976).
38. J. P. Lewis, J. H. Goodykoontz and J. F. Kline, Boiling heat transfer to liquid hydrogen and nitrogen in forced flow, NASATN D-1314 (1962).
39. S. S. Papell, Combined buoyancy and flow direction effects on saturated boiling critical heat flux in liquid nitrogen, *Adv. Cryogen. Engng* **18**, 65–72 (1972).
40. G. F. Stevens, D. F. Elliot and R. W. Wood, An experimental investigation into forced convection burnout in Freon, with reference to burn-out in water, uniformly heated round tubes with vertical up-flow, UKAEA, AEEW-R 321 (1964).
41. G. F. Stevens, D. F. Elliot and R. W. Wood, An experimental comparison between forced convection burn-out in Freon 12 flowing vertically upwards through uniformly and non-uniformly heated round tubes, UKAEA, AEEW-R 426 (1965).
42. P. G. Barnett and R. W. Wood, An experimental investigation to determine the scaling laws of forced convection boiling heat transfer, Part 2, UKAEA, AEEW-R 443 (1965).
43. D. C. Groeneveld, The occurrence of upstream dryout in uniformly heated channels, *Heat Transfer 1974*, Vol. 4, pp. 265–269. Hemisphere, Washington (1974).
44. M. Cumo, R. Bertoni, R. Cipriani and G. Palazzi, Up-flow and down-flow burnout, *Inst. Mech. Engrs Conference Publications* 1977–8, pp. 183–192 (1977).
45. F. W. Staub, Two-phase fluid modeling – the critical heat flux, *Nucl. Sci. Engng* **35**, 190–199 (1969).
46. R. D. Coffield, Jr., W. M. Rohrer, Jr. and L. S. Tong, A subcooled DNB investigation of Freon-113 and the similarity to subcooled water DNB data, *Nucl. Engng. and Design* **11**, 143–153 (1969).
47. T. Ueda, H. Tanaka and Y. Koizumi, Dryout of liquid film in high quality R-113 upflow in a heated tube, in *Heat Transfer 1978*, Vol. 1, pp. 423–428. Hemisphere, Washington (1978).
48. Y. Koizumi, T. Ueda and H. Tanaka, Post dryout heat transfer to R-113 upward flow in a vertical tube, *Int. J. Heat Mass Transfer* **22**, 669–678 (1979).
49. G. E. Dix, Freon-water modeling of CHF in round tubes, ASME Paper No. 70-HT-26 (1970).
50. H. W. Hoffman and A. I. Krakoviak, Convection boiling with liquid potassium, *Proceedings of the 1964 Heat Transfer and Fluid Mechanics Institute*, pp. 19–37. Stanford Univ. Press, Stanford (1964).
51. J. A. Bond and G. L. Converse, Vaporization of high-temperature potassium in forced convection at saturation temperatures of 1800° to 2100°F, NASA CR-843 (1967).
52. T. Alad'yev, I. G. Gorlov, L. D. Dodonov and O. S. Fedynskiy, Heat transfer to boiling potassium in uniformly heated tubes, *Heat Transfer–Soviet Res.* **1**(4), 14–26 (1969).
53. S. C. Cheng and W. Ng, Transition boiling heat transfer in forced vertical flow via a high thermal capacity heating process, *Letters in Heat and Mass Transfer* **3**, 333–342 (1976).
54. V. M. Borishansky, A. A. Andreevsky, G. S. Bykov, V. A. Shleifer, M. E. Lebedev and M. J. Belenky, The heat transfer crisis at the steam water flowing in channels in high steam content zones, *Heat Transfer 1974*, Vol. IV, pp. 285–289. Hemisphere, Washington (1974).
55. V. E. Doroshchuk and F. P. Lantsman, Effect of pressure and mass flow rate on burnout heat flux in a water and steam–water mixture flow in tubes, *Int. J. Heat Mass Transfer* **7**, 187–190 (1964).
56. V. N. Smolin, Boiling heat transfer crisis in tubes with dispersed-annular flow of steam–water mixtures, *Heat Transfer 1970*, Vol. VI, B.6.8. Elsevier, Amsterdam (1970).
57. T. C. Core and K. Sato, Determination of burnout limits of polyphenyl coolants. AEC Research and Development Report, IDO-28007 (1958).
58. W. R. Gambill, How to estimate engineering properties, *Chem. Engng*, 261–266 (Dec. 1957), 195–202 (Oct. 19, 1959), 146–150 (Apr. 7, 1958), 263–268 (July 1957).
59. J. C. Collier, *Convection Boiling and Condensation*, p. 240. McGraw-Hill, New York (1972).
60. W. M. Rohsenow and J. P. Hartnett (editors), *Handbook of Heat Transfer*, Section 13. McGraw-Hill, New York (1973).
61. M. Monde and Y. Katto, Burnout in a high heat-flux boiling system with an impinging jet, *Int. J. Heat Mass Transfer* **21**, 295–305 (1978).
62. Y. Katto and K. Ishii, Burnout in a high heat flux boiling system with a forced supply of liquid through a plane jet, in *Heat Transfer 1978*, Vol. 1, pp. 435–440. Hemisphere, Washington (1978).
63. Y. Katto and M. Shimizu, Upper limit of CHF in the saturated forced convection boiling on a heated disk with a small impinging jet, *J. Heat Transfer* **101***C*, 265–269 (1979).
64. J. P. Lienhard and R. Eichhorn, On predicting boiling burnout for heaters cooled by liquid jets, *Int. J. Heat Mass Transfer* **22**, 774–776 (1979).

ASPECT GENERAL DU FLUX CRITIQUE EN CONVECTION FORCEE DANS DES TUBES VERTICAUX, CHAUFFES, AVEC UN SOUS-REFROIDISSEMENT NUL A L'ENTREE

Résumé — On développe une méthode graphique qui, en un clin d'oeil, rassemble les données connues pour le flux critique (CHF) dans les tubes verticaux, sans sous-refroidissement à l'entrée. On utilise 946 points expérimentaux provenant de 47 sources et concernant 14 fluides (eau, ammoniac, benzène, éthanol, freons, helium I, parahydrogène, monoisopropylbiphenyl, azote et potassium), une longueur de tube allant de 0,0109 à 8,82 m, un diamètre de tube de 0,00027 à 0,413. On dégage une nature régulière du flux critique.

HAUPTMERKMALE DER KRITISCHEN WÄRMESTROMDICHTE (KWD) BEIM SIEDEN BEI ERZWUNGENER KONVEKTION IN GLEICHFÖRMIG BEHEIZTEN SENKRECHTEN ROHREN BEI EINER EINTRITTSUNTERKÜHLUNG VON NULL

Zusammenfassung—In diesem Aufsatz wird eine grafische Methode entwickelt, um einen allgemeinen Überblick über die vorhandenen Daten für die KWD in senkrechten Rohren bei einer Anfangsunterküblung von null zu geben. Zu diesem Zweck wurden 946 Versuchsergebnisse aus 47 Quellen verwendet. Diese umfassen 14 verschiedene Flüssigkeiten (Wasser, Ammoniak, Benzol, Äthanol, Freone, Helium I, Parawasserstoff, Monoisopropylbiphenyl, Stickstoff und Kalium), Rohrlängen von 0,0109 bis 8,82 m, Rohrdurchmesser von 0,00109 bis 0,0381 m und Dampf/Flüssigkeit-Dichteverhältnisse von 0,000270 bis 0,413. Als Ergebnis wird ein regulärer Verlauf der untersuchten KWD erhalten.

КРИТИЧЕСКИЕ ТЕПЛОВЫЕ ПОТОКИ ПРИ КИПЕНИИ В УСЛОВИЯХ ВЫНУЖДЕННОЙ КОНВЕКЦИИ В РАВНОМЕРНО НАГРЕВАЕМЫХ ВЕРТИКАЛЬНЫХ ТРУБАХ ПРИ ОТСУТСТВИИ НЕДОГРЕВА НА ВХОДЕ

Аннотация — Предложен графический метод обобщения имеющихся данных по критическому тепловому потоку в вертикальных трубах при отсутствии недогрева на входе. С этой целью использовано 946 экспериментальных точек из 47 источников для 14 различных жидкостей (вода, аммиак, бензол, этанол, фреоны, гелий-I, параводород, моноизопропилбифенил, азот и калий) в трубах длиной от 0,0109 до 8,82 м, диаметром от 0,00109 до 0,0381 м при отношениях плотности пара к плотности жидкости в пределах 0,000270–0,413. Выявлены закономерности для критического теплового потока в исследуемом диапазоне параметров.